

SNARE-RNAi Results in Higher Terpene Emission from Ectopically Expressed Caryophyllene Synthase in *Nicotiana benthamiana*

Hieng-Ming Ting¹, Thierry L. Delatte¹, Pim Kolkman¹, Johana C. Misas-Villamil², Renier A.L. van der Hoorn^{2,3}, Harro J. Bouwmeester¹ and Alexander R. van der Krol^{1,*}

¹Laboratory of Plant Physiology, Wageningen University, PO Box 658, 6700 AR Wageningen, The Netherlands

²Plant Chemetics Laboratory, Max Planck Institute for Plant Breeding Research, Carl-von-Linne Weg 10, 50829 Cologne, Germany

³Plant Chemetics Laboratory, Department of Plant Sciences, University of Oxford, South Parks Road, Oxford OX1 3RB, UK

*Correspondence: Alexander R. van der Krol (sander.vanderkrol@wur.nl)

<http://dx.doi.org/10.1016/j.molp.2015.01.006>

ABSTRACT

Plants produce numerous terpenes and much effort has been dedicated to the identification and characterization of the terpene biosynthetic genes. However, little is known about how terpenes are transported within the cell and from the cell into the apoplast. To investigate a putative role of vesicle fusion in this process, we used *Agrobacterium tumefaciens*-mediated transient coexpression in *Nicotiana benthamiana* of an *MtVAMP721e-RNAi* construct (*Vi*) with either a caryophyllene synthase or a linalool synthase, respectively. Headspace analysis of the leaves showed that caryophyllene or linalool emission increased about five-fold when *N. benthamiana* VAMP72 function was blocked. RNA sequencing and protein ubiquitination analysis of the agroinfiltrated *N. benthamiana* leaf extracts suggested that increased terpene emissions may be attributed to proteasome malfunction based on three observations: leaves with *TPS+Vi* showed (1) a higher level of a DsRed marker protein, (2) a higher level of ubiquitinated proteins, and (3) coordinated induced expression of multiple proteasome genes, presumably caused by the lack of proteasome-mediated feedback regulation. However, caryophyllene or linalool did not inhibit proteasome-related protease activity in the *in vitro* assays. While the results are not conclusive for a role of vesicle fusion in terpene transport, they do show a strong interaction between inhibition of vesicle fusion and ectopic expression of certain terpenes. The results have potential applications in metabolic engineering.

Key words: terpene transport, vesicle-associated membrane proteins (VAMP72), caryophyllene synthase, linalool synthase, proteasome, *Nicotiana benthamiana*

Ting H.-M., Delatte T.L., Kolkman P., Misas-Villamil J.C., van der Hoorn R.A.L., Bouwmeester H.J., and van der Krol A.R. (2015). SNARE-RNAi Results in Higher Terpene Emission from Ectopically Expressed Caryophyllene Synthase in *Nicotiana benthamiana*. *Mol. Plant*. **8**, 454–466.

INTRODUCTION

Plants produce numerous volatile terpenoids, which have many different functions, varying from plant hormones to abiotic stress protectants (e.g. heat protection) or in biotic stress responses (e.g. attraction of predators of plant herbivores) (Holopainen and Gershenzon, 2010). Emission of volatile terpenes from plant cells may involve multiple pathways, e.g. (1) insertion of the hydrophobic terpene into vesicle membranes followed by transport and fusion to the plasma membrane, (2) carrier proteins that transport these molecules to the (plasma) membrane (e.g. similar to the role of GST proteins in flavonoid transport; Zhao and Dixon, 2010), (3) membrane ABC transporters involved in the translocation of terpenes over the

plasma membrane, and (4) potential direct diffusion between the endoplasmic reticulum (ER) and/or plastidial (stromule) membranes and the plasma membrane, possibly through specific contact sites. Multiple transport pathways have also been described for the transport of non-volatile lipids, involving both a vesicle and non-vesicular transport mechanism (Lev, 2010).

As lipophilic compounds would favor sequestering into membranes, one option for the transport of terpenes within the cell

could be through vesicle transport between subcellular compartments and delivery of the terpenoids to target membranes by vesicle fusion. Hints that terpenoids may be transported by vesicles come from studies on *Plasmodium falciparum*, for which it was shown that the sesquiterpene lactone artemisinin is transported from the red blood cell into the parasite (*P. falciparum*) via parasite-derived membrane vesicles (Eckstein-Ludwig et al., 2003; Gershenzon and Dudareva, 2007). A study on *Sauromatum guttatum* flowers showed fusion of vesicles from the ER with the plasma membrane, and this correlated with the heat-induced release of sesquiterpenes (α -copaene and caryophyllene) (Skubatz et al., 1995), hinting at the involvement of vesicle transport and fusion in terpene emission. The results from this study may be an indication that terpenes are stored in vesicles which are transported to the plasma membrane and that, supposedly, fusion of these vesicles with the plasma membrane results in the release of the volatile sesquiterpenes. The fusion of vesicles with target membranes is mediated by a group of proteins called SNAREs (Soluble N-ethylmaleimide sensitive factor Attachment protein REceptor) (Lang and Jahn, 2008). One v-SNARE (SNARE protein on the transport vesicle) pairs with three t-SNARE proteins (SNARE proteins on the target membrane, including syntaxins) (Lang and Jahn, 2008), leading to membrane fusion between the two compartments. v-SNAREs consist of long vesicle-associated membrane proteins (VAMPs) or “longins” (containing an N-terminal longin domain) and short VAMPs or “brevins” (Filippini et al., 2001). However, in plants only the longin-type v-SNAREs occur, and they can be further classified into three major groups: VAMP7-like, Ykt6-like, and Sec22-like (Fujimoto and Ueda, 2012). A subgroup of the VAMP7-likes, the VAMP72 family, has been shown to be involved in exocytosis in plants (Sanderfoot, 2007; Kwon et al., 2008), while a VAMP72 protein from *Medicago truncatula* (MtVAMP721) was shown to be involved in the exocytosis pathway required for arbuscule formation (Ivanov et al., 2012).

Here we addressed the questions whether vesicle transport is involved in the transport of terpenoids within the cell and whether vesicle fusion plays a role in the emission of the terpenoids into the apoplast. As a model we used the volatile sesquiterpene caryophyllene, which is not easily converted to oxidized and/or glycosylated, non-volatile, compounds upon ectopic production in plants, and the monoterpene linalool. To evaluate the role of vesicle transport/fusion we combined transient expression of caryophyllene synthase (CST) or linalool synthase (FaNES) with a SNARE-RNAi construct targeted at *N. benthamiana* VAMP72 genes. Surprisingly, the coexpression of CST (C) with MtVAMP721e-RNAi (Vi) resulted in five-fold higher caryophyllene emission levels. Sequence analysis of RNA from samples with C+Vi showed a stronger transcriptional response than C or Vi alone. Specifically a coordinated upregulation of genes encoding components of the 26S proteasome was noted, which may be a hallmark of reduced negative feedback on proteasome gene expression when proteasome functionality is impaired (Kobayashi and Yamamoto, 2005; Villeneuve et al., 2010). Indeed, higher levels of ubiquitinated proteins were found in extracts from the CST+MtVAMP721e-RNAi agroinfiltrated leaves, indicating that reduced protein turnover may be a cause of the higher terpene production. However, caryophyllene did not inhibit protease activity of proteasomes in an *in vitro* assay.

Results are discussed in the context of the different pathways that may be involved in terpene emission.

RESULTS

Expression of VAMP72-RNAi Enhances Transient Caryophyllene Production

For the production of the volatile sesquiterpene caryophyllene in plants, a fragment of *Arabidopsis* genomic DNA was isolated, encoding the caryophyllene synthase (CST) TPS21, and this fragment was fused to the constitutive CaMV35S promoter in a construct we used for transient expression in *N. benthamiana*. Caryophyllene production was assayed by a headspace trapping assay for isolated leaves, harvested at 7 days post agroinfiltration. Pilot studies indicated that substantial amounts of caryophyllene are produced by leaves agroinfiltrated with the 35S:CST (C) construct (data not shown). For the inhibition of VAMP72 gene expression in *N. benthamiana*, we used the MtVAMP721e-RNAi (Vi) expression construct previously described to inhibit vesicle transport in *M. truncatula* (Ivanov et al., 2012). We identified 14 VAMP72 genes in *N. benthamiana*, and sequence analysis of the *N. benthamiana* genome showed 14 VAMP72-like genes with 67%–83% DNA sequence identity to MtVAMP721e, with highest DNA sequence identity to NbVAMP72c (Supplemental Figures 1A and 2A). The MtVAMP721e-RNAi (Vi) was transiently expressed in *N. benthamiana* leaves and RNA was isolated at 7 days post agroinfiltration. Quantitative reverse transcription PCR (qRT-PCR) analysis using MtVAMP72c-specific primers indicated that the transient expression of Vi reduced VAMP72c mRNA levels almost nine-fold compared with the control (Supplemental Figure 2B), indicating that the heterologous MtVAMP721e-RNAi can efficiently target *N. benthamiana* VAMP72 genes. Because the high levels of RNAi in transient expression may generate pleiotropic effects on gene silencing (e.g. by titration of Argonaute complexes), we also tested the effect of a DsRed-RNAi (Di) construct in combination with 35S:CST (C). Note that all vectors containing an RNAi construct also contained a DsRed marker gene (Figure 1).

For all the different treatments the relative dosage of C and Vi was kept constant by combining expression with Di. For Di the relative gene dosage was kept constant by combining expression with an empty vector (*pBin*: P). To determine the effect on headspace emission of caryophyllene, we compared the treatments *pBin*+DsRed-RNAi (P+Di), MtVAMP721e-RNAi+DsRed-RNAi (Vi+Di), CST+DsRed-RNAi (C+Di), and CST+MtVAMP721e-RNAi (C+Vi). All treatments were evaluated at 7 days post agroinfiltration by harvesting the infiltrated leaves and measuring the amount of caryophyllene released into the headspace in 30 min in the light. As expected, leaves transiently expressing P+Di or Vi+Di produced only very low levels of caryophyllene, which can be attributed to endogenous *N. benthamiana* CST activity (Figure 2). However, leaves with C+Di produced substantial amounts of caryophyllene in the 30 min of headspace trapping (Figure 2). One could expect that if vesicle fusion is involved in caryophyllene transport, inhibition of vesicle fusion by downregulation of VAMP72 expression would decrease the emission of caryophyllene. However, in the C+Vi treated leaves the caryophyllene emission was approximately five-fold higher (Figure 2). This indicates that inhibition of *N. benthamiana*

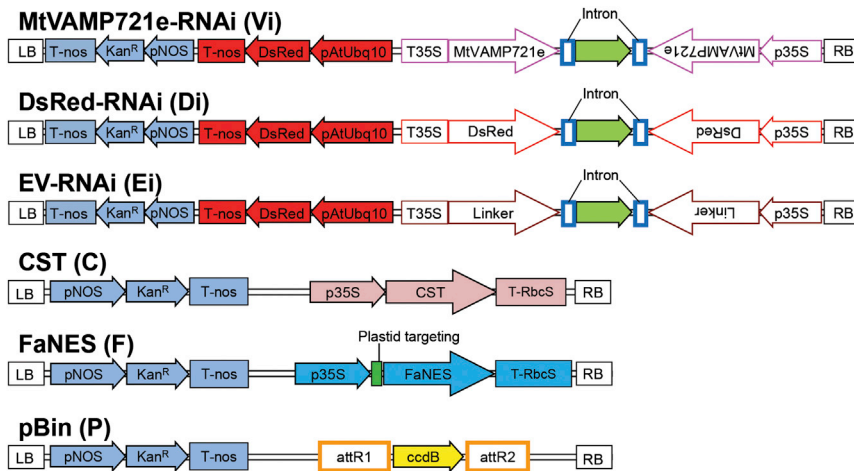


Figure 1. Maps of Constructs Used in this Study.

attR1-attR2, recombination sites for LR reaction; *ccdB*, negative bacterial selection marker; *Cm^R*, chloramphenicol resistance; *Kan^R*, kanamycin resistance; *p35S*, CaMV35S promoter; *pAtUbg10*, *Arabidopsis Ubiquitin10* promoter; *pNOS*, promoter of nopaline synthase gene; *T-nos*, terminator of nopaline synthase gene.

VAMP72 gene expression does affect the flux through the caryophyllene emission pathway, but in an unexpected way. In total, the experiment was repeated six times, every time yielding similar results. To understand better why the C+Vi treatment resulted in higher caryophyllene emission levels, we chose to perform RNA sequencing (RNA-seq) on the different leaf samples to investigate the transcriptional response to the different agroinfiltration treatments.

RNA-Seq Analysis of Agroinfiltrated Leaves

To better understand how the inhibition of vesicle transport, when combined with *CST*, leads to enhanced caryophyllene emission, we performed semi-quantitative sequence analysis on RNA isolated from the agroinfiltrated leaves. For this, RNA was extracted from the leaves at 7 days post agroinfiltration of the combinations *P+Di*, *Vi+Di*, *C+Di*, and *C+Vi* for quantification by RNA-seq (see Methods). The relative expression levels of genes were compared with that of the control treatment (*P+Di*) and differentially expressed genes between *Vi+Di*, *C+Di*, or *C+Vi* and the control were selected, using a threshold of the absolute value of $\log_2\text{FoldChange} \geq 1$ at a false discovery rate (FDR) ≤ 0.05 . Figure 3A shows the total transcriptional response of differentially expressed genes and the treatment-specific response (total differential transcriptional response minus the overlap with either of the other two treatments). Results show that inhibition of vesicle fusion (treatment *Vi+Di*) caused upregulation of only 144 and downregulation of 214 genes (Figure 3A). The transcriptional response to caryophyllene overproduction (treatment *C+Di*) was more pronounced, with 619 upregulated and 769 downregulated genes compared with *P+Di*. By contrast, the transcriptional response to the combination of caryophyllene overproduction with inhibition of *VAMP72* activity (treatment *C+Vi*) resulted in the upregulation of 1822 genes and downregulation of 1353 genes compared with the control. Also, when corrected for the overlap in transcriptional response, the coexpression of *CST* and *MtVAMP721e-RNAi* causes a much larger change in the gene expression profile (1400 upregulated, 1192 downregulated) than the specific response to either *Vi+Di* (49 upregulated, 63 downregulated) or *C+Di* (412 upregulated, 454 downregulated) (Figure 3A). The Venn diagrams of the overlap in transcriptional response for the different treatments are shown in Figure 3B. To gain insight into the biological processes affected by the different treatments, a gene ontology

(GO)-term enrichment analysis was performed on the differentially expressed genes, using $P \leq 0.05$ (Supplemental Tables 1–3). In addition, the differentially expressed genes of the different treatments were mapped to the reference

canonical plant pathways in the Kyoto Encyclopedia of Genes and Genomes (KEGG) (Supplemental Tables 4–6). For each of the three treatments, the top 10 pathways that were most affected are shown in Supplemental Table 7. The pathways that were most strongly affected by the different treatments were also visualized via the MapMan tool (Thimm et al., 2004). An overview of all differentially expressed genes between *Vi+Di*, *C+Di*, and *C+Vi* versus control *P+Di* for cellular metabolism is shown in Supplemental Figure 3. A list of all up- or downregulated differentially expressed genes corresponding to MapMan functional categories is provided in Supplemental Table 8.

Transcriptional Response to *Vi+Di* Treatment

Analysis of the differentially expressed genes that are specific for *MtVAMP721e-RNAi* shows that the *VAMP72* genes of *N. benthamiana* are most strongly affected (as expected). As a result, the SNARE interaction pathway of vesicular transport shows up for this treatment as the pathway that is strongly affected (Supplemental Table 7). Supplemental Figure 1B shows the average number of RNA reads for each member of the *VAMP72* gene family in *N. benthamiana*, for each of the treatments. Results indicate that in 10 of the 14 different *N. benthamiana* *VAMP72* genes the expression was downregulated in leaf samples agroinfiltrated with the *MtVAMP721e-RNAi* construct (*Vi+Di* or *C+Vi*). This indicates that the *M. truncatula* *MtVAMP721e-RNAi* targets multiple *VAMP72* genes in *N. benthamiana*, but other *VAMP* genes (e.g. *VAMP71* gene family members) are not affected by either the *Vi+Di* or *C+Vi* treatment. Using the threshold of $Q \leq 0.05$, other pathways were not significantly affected by *Vi+Di* (Supplemental Table 7). Supplemental Figure 3A shows the MapMan projection of differentially expressed genes for cellular metabolism, indicating that no major pathway was affected by the *Vi+Di* treatment. Details of the GO classification of differentially expressed genes are given in Supplemental Tables 1–3. Details of the KEGG enrichment analysis for the *Vi+Di* treatment are given in Supplemental Table 4.

Transcriptional Response to *C+Di* Treatment

Analysis of the transcriptional response to *CST* indicates that ectopic production of caryophyllene creates a substantial pleiotropic effect in leaves (Supplemental Table 7). GO-term

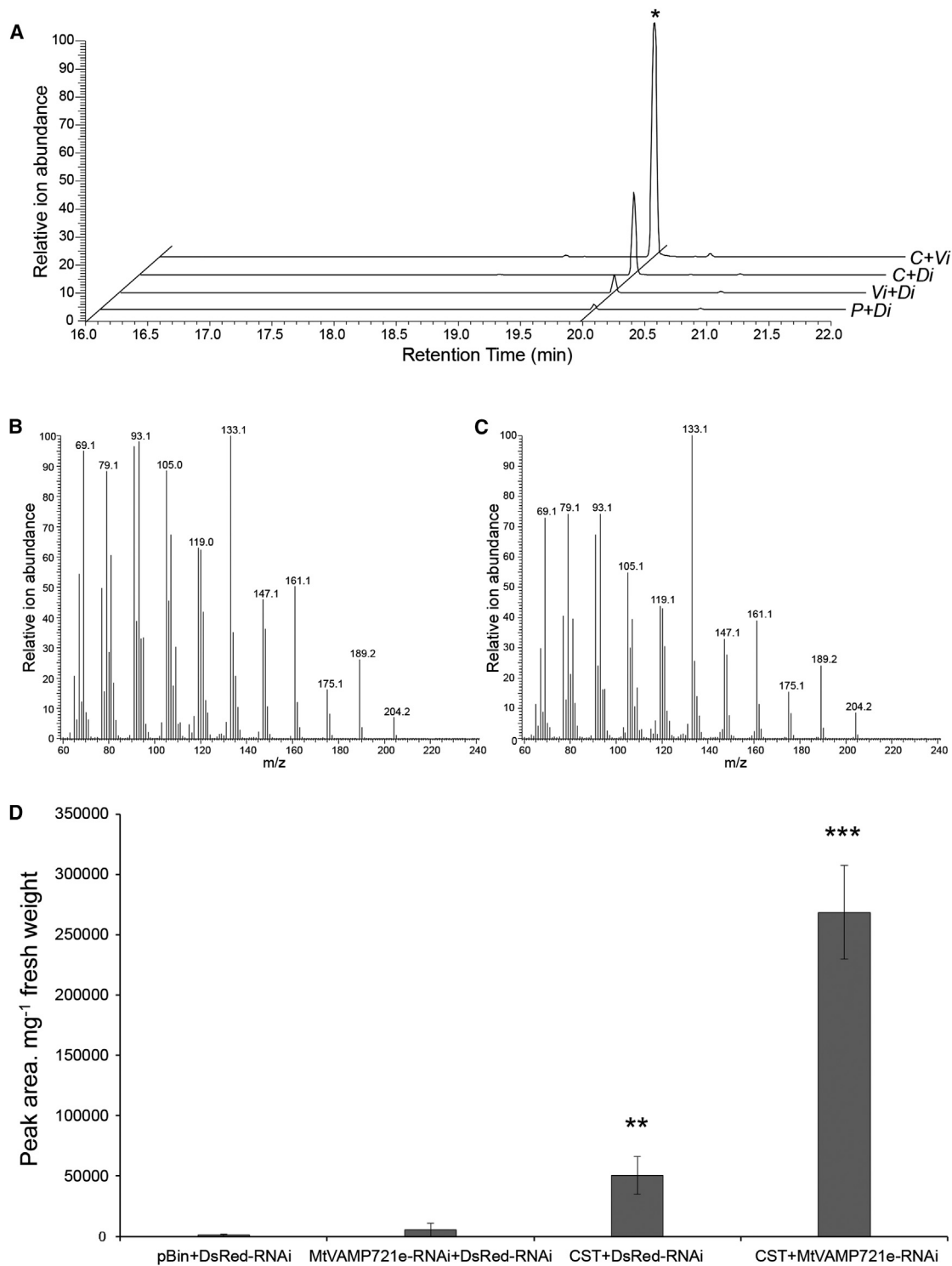


Figure 2. Caryophyllene Emission from *Nicotiana benthamiana* Leaves.

(A) GC–MS chromatograms showing the caryophyllene emitted from *N. benthamiana* transiently expressing *pBin+DsRed-RNAi* (*P+Di*), *MtVAMP721e-RNAi+DsRed-RNAi* (*Vi+Di*), *CST+DsRed-RNAi* (*C+Di*), and *CST+MtVAMP721e-RNAi* (*C+Vi*). *Caryophyllene.

(B) Mass spectrum of caryophyllene emitted by *N. benthamiana*.

(C) Mass spectrum of caryophyllene standard.

(D) Peak area of caryophyllene produced by leaves of *N. benthamiana*, as detected by headspace GC–MS analysis. Each bar represents the mean of three biological replicates \pm SE. Statistically significant differences between control (*P+Di*) and treatments (*Vi+Di*, *C+Di*, and *C+Vi*) are indicated by asterisks (Student’s *t*-test: ** $P < 0.01$; *** $P < 0.001$).

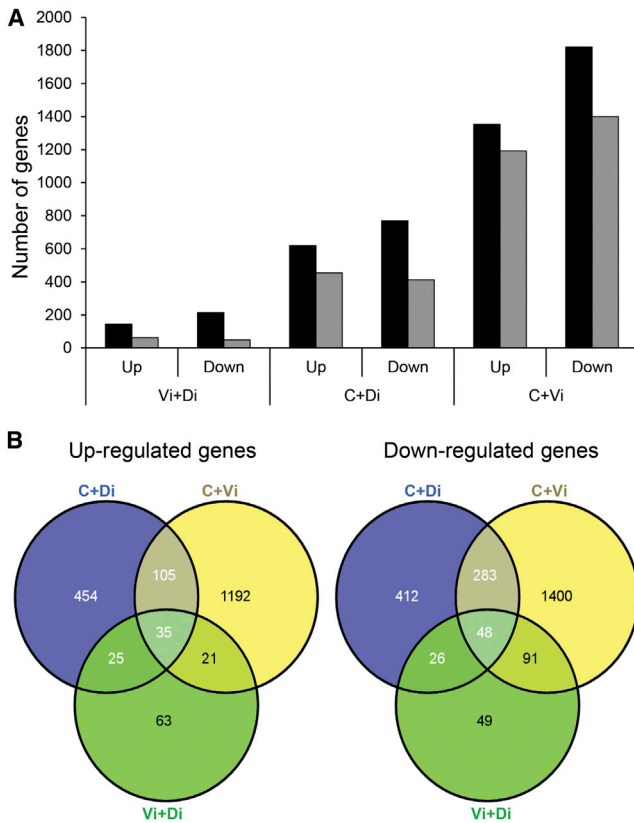


Figure 3. Overview of Transcriptional Response Relative to the *pBin+DsRed-RNAi* (*P+Di*) Treatment.

(A) Total (black) and treatment-specific (gray) gene response relative to *P+Di*. Treatment-specific response = total response minus overlap with either of the other treatments.

(B) Venn diagrams showing common genes significantly up- and down-regulated in *N. benthamiana* leaves transiently expressing *Vi+Di*, *C+Di*, or *C+Vi* compared with leaves infiltrated with *P+Di* (cut-off \log_2 FoldChange ≥ 1 and false discovery rate ≤ 0.05).

Vi+Di, *MtVAMP721e-RNAi+DsRed-RNAi*; *C+Di*, *CST+DsRed-RNAi*; *C+Vi*, *CST+MtVAMP721e-RNAi*.

enrichment analysis of the specific differentially expressed genes in the *C+Di* treatment shows that glucan metabolic processes in cell periphery and cell wall are affected by the ectopic caryophyllene production. In addition, ectopic production of caryophyllene had a strong negative effect on the expression of genes involved in glycosaminoglycan degradation, suggesting a reduced breakdown of glycosaminoglycans. Projection of the data in MapMan shows that *C+Di* also resulted in downregulation of genes involved in cell wall biosynthesis (Supplemental Figure 3B), while biotic response, heat stress response, calcium signaling, and development genes were significantly induced (Supplemental Table 8). Details of the GO classification of differentially expressed genes are given in Supplemental Tables 1–3. Details of the KEGG enrichment analysis for the *C+Di* treatment are given in Supplemental Table 5.

Transcriptional Response to the *C+Vi* Treatment

CST was a component of the *C+Di* and *C+Vi* treatments, both having the same dosage of the *CST* expression construct in the agroinfiltration. Using the cut-off value \log_2 FoldChange ≥ 1 , the

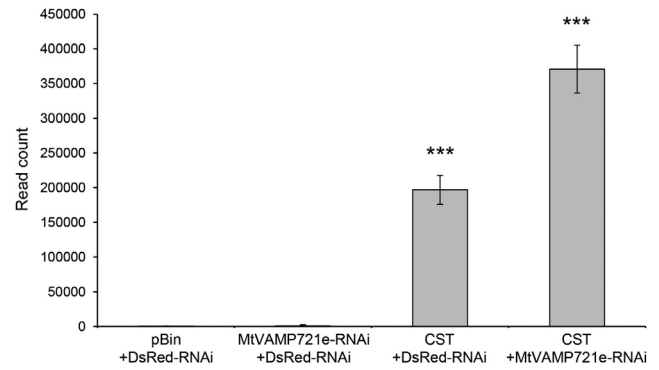


Figure 4. Total Number of *CST* Reads in Leaves Agroinfiltrated with *pBin+DsRed-RNAi*, *MtVAMP721e-RNAi+DsRed-RNAi*, *CST+DsRed-RNAi*, and *CST+MtVAMP721e-RNAi*.

All RNA-seq data were based on three independent replicates. Error bars indicate standard deviation. Statistically significant differences between control (*pBin+DsRed-RNAi*) and treatments (*MtVAMP721e-RNAi+DsRed-RNAi*, *CST+DsRed-RNAi*, and *CST+MtVAMP721e-RNAi*) are indicated by asterisks (Student's *t*-test: ****P* < 0.001).

CST transgene was not part of the differentially expressed genes. Although the read counts of *CST* in the *C+Di* and *C+Vi* treatments indicated a slightly higher count in the *C+Vi* treatment (1.8-fold) (Figure 4), this is not sufficient to account for the five-fold increased emission of caryophyllene in this treatment (Figure 2). In the RNA reads we can distinguish between the *Arabidopsis* *CST* sequence and *N. benthamiana* *CST* genes. *N. benthamiana* has six genes with close homology to *Arabidopsis* *CST*. Curiously, the number of RNA reads specific for these endogenous *NbCST* homologs were actually more than two-fold down in *C+Di* and *C+Vi* compared with the *P+Di* treatment (Supplemental Figure 4).

When caryophyllene production was combined with inhibition of VAMP72 function, some of the specific transcriptional responses to *CST* alone were abolished. For instance, compared with the *C+Di* treatment, the *C+Vi* treatment does no longer show a significant increase in differentially expressed genes involved in biotic stress, heat stress, and calcium signaling (Supplemental Table 8). Most interestingly, the combination *C+Vi* specifically upregulates processes related to protein turnover by the 26S proteasome complex and downregulates processes related to photosynthesis (Supplemental Table 1). Visualization of the output of KEGG for the ubiquitin-dependent degradation pathway shows specific upregulation for the *C+Vi* treatment of almost every gene-encoding component of the proteasome. These include 14 of 14 components of the proteasome core, 6 of 9 components of the proteasome lid, and 7 of 9 components of the proteasome base (Figure 5). None of the upregulated genes were affected by the *C+Di* treatment and only one gene was affected by the *Vi+Di* treatment (proteasome lid subunit N6 was downregulated both in *C+Vi* and *Vi+Di* compared with control *P+Di*).

Analysis of the data shows that genes involved in cell wall-related processes also were downregulated in the *C+Vi* treatment (Supplemental Figure 3C). We performed a Wilcoxon rank-sum test of differentially expressed genes for the treatments (Supplemental Table 8), which shows that some genes of the

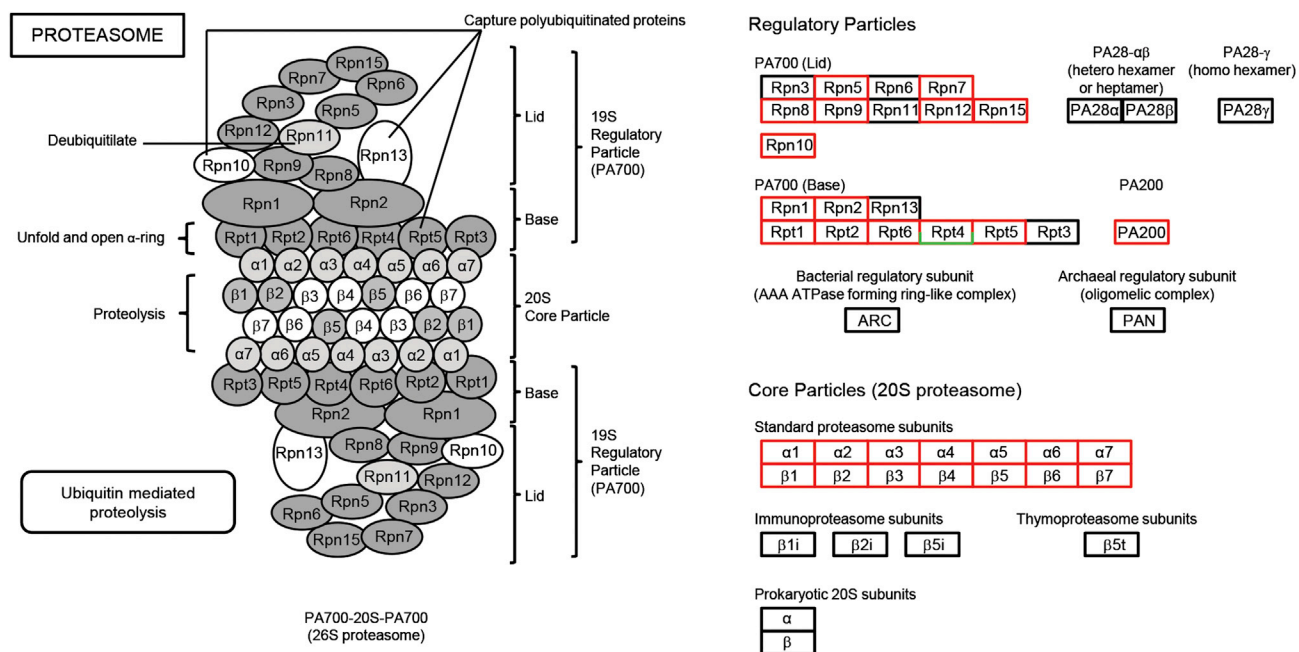


Figure 5. Proteasome Genes in Leaves Agroinfiltrated with *CST+MtVAMP721e-RNAi* that Were Differentially Expressed Were Mapped in the KEGG Pathway.

The green and red boxes indicate up- or downregulation of a gene or a group of genes that is mapped to that category. Boxes with half green and half red indicate the presence of genes that showed down- or upregulation and were mapped to the category of gene in the map.

phenylpropanoid pathway (mainly lignin biosynthesis) showed reduced expression (Supplemental Table 8, bin 16.2). Besides the many genes involved in cellular processes for which expression was downregulated by the C+Vi treatment, a number of transcription factors were upregulated by this treatment (e.g. AP2/EREBP, C2C2(Zn) CO-like, MADS box transcription factor family) (Supplemental Table 8, bins 27.3.3, 27.3.7, and 27.3.24). The upregulation of these transcription factors may explain why so many more genes are affected in the C+Vi treatment compared with the other treatments (Vi+Di, C+Di) in which just a few transcription factors were induced (Figure 3 and Supplemental Table 8). Details of the GO classification of differentially expressed genes are given in Supplemental Tables 1–3. Details of the KEGG enrichment analysis for the C+Vi treatment are given in Supplemental Table 6, and details of the Wilcoxon rank-sum test of differentially expressed genes are given in Supplemental Table 8.

Indications of Reduced Proteasome Activity in C+Vi Treatment

Results from the transcriptional response to *CST+MtVAMP721e-RNAi* (C+Vi) indicate a coordinated upregulation of genes encoding the lid, base, and core particle of the 26S proteasome complex. From yeast and mammalian studies it is known that transcriptional control of proteasome genes is under feedback regulation by a transcription factor (NF-E2-related factor 2, Nrf2), which itself is targeted for degradation by the 26S proteasome (Kobayashi and Yamamoto, 2005). When proteasome function is impaired, the activity of this transcription factor increases and, consequently, so does the expression of proteasome genes (Meiners et al., 2003). Although such

feedback regulation has not yet been described for plants, the upregulation of proteasome gene expression in response to the C+Vi treatment in *N. benthamiana* (Figure 5) could be indicative of reduced proteasome activity. If indeed proteasome function is impaired in the C+Vi treatment, this could then also account for the higher caryophyllene emissions if enzymes in the caryophyllene biosynthesis pathway display higher protein stability.

The *DsRed* gene is part of all RNAi constructs, but the treatments P+Di, Vi+Di, and C+Di also contain a *DsRed-RNAi* construct. Indeed, in these treatments the expression level of *DsRed* was low, while the number of counts for *DsRed* RNA was high in the C+Vi treatment (data not shown).

To obtain further information on possible effects on protein stability in the C+Vi treatments, we analyzed the effect on DsRed protein accumulation. In a separate experiment we tested the effect of an empty RNAi vector (*Ei*, which only contains a small linker) on CST activity. Leaves transiently expressing C+*Ei* emitted levels of caryophyllene similar to those of C+Di, while again C+Vi stimulated caryophyllene emission (Figure 6A; compare with Figure 2). Because both the *Ei* and Vi vector contain the 35S:*DsRed* gene, we now could also compare the accumulation of DsRed protein in the combinations C+*Ei* and C+Vi. Leaves infiltrated with C+Vi visually had a higher DsRed level than in the empty vector control (Figure 6B). Semi-quantification of the signal in the red and green components of the images, setting the average signal for the red (DsRed) and green (chlorophyll) channel of the C+*Ei* image at 100%, showed a significant increase of about 25% for the red signal in the C+Vi treatment (Figure 6C), indicating reduced turnover of the DsRed

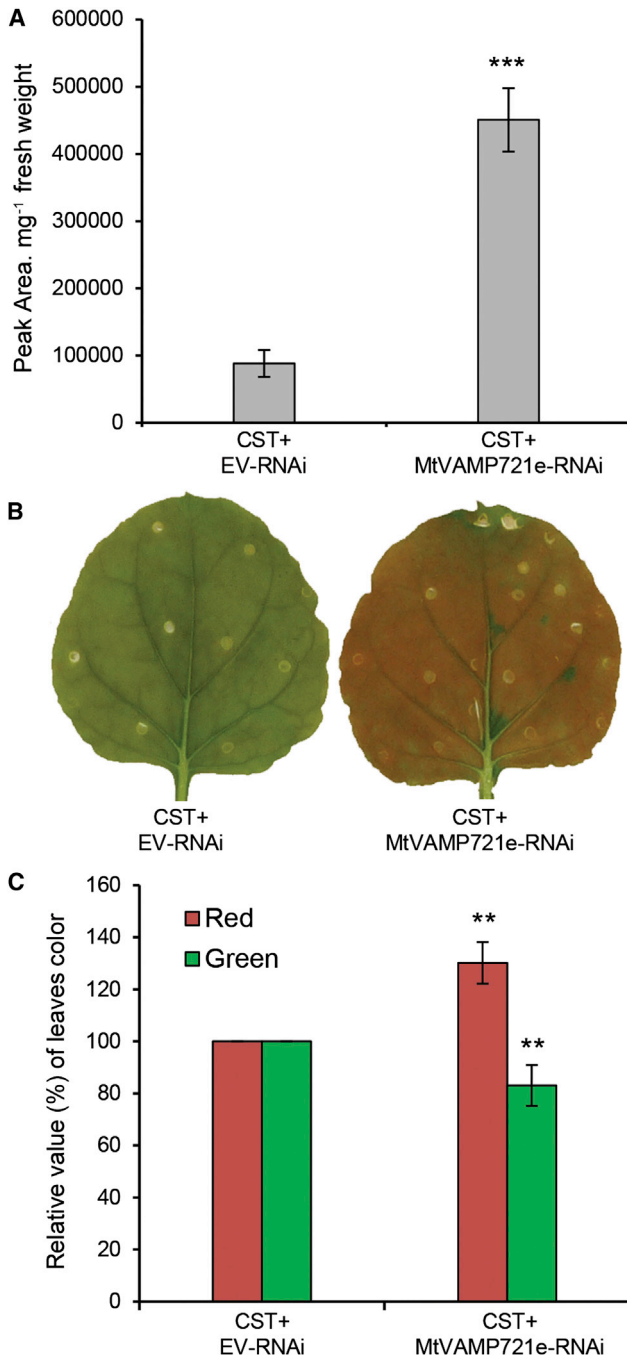


Figure 6. Caryophyllene Emission and DsRed Stabilization in *CST+MtVAMP721e-RNAi* Agroinfiltrated Leaves.
(A) Caryophyllene emission in leaves agroinfiltrated with *CST+EV-RNAi* and *CST+MtVAMP721e-RNAi*.
(B) Coloration of leaves 7 days post agroinfiltration with *CST+EV-RNAi* and *CST+MtVAMP721e-RNAi*.
(C) Quantification of relative red and green signal intensities in **(B)**. In **(A)** and **(C)**, each bar represents the mean of three biological replicates ± SE. Statistically significant differences between *CST+EV-RNAi* and *CST+MtVAMP721e-RNAi* are indicated by asterisks (Student's *t*-test: ***P* < 0.01; ****P* < 0.001).

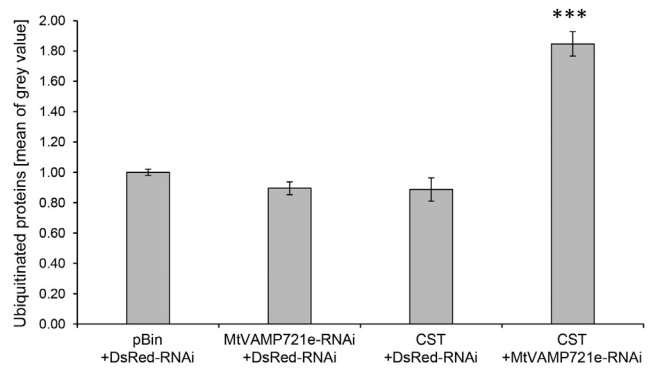


Figure 7. Protein Ubiquitination Levels in Agroinfiltrated Leaves.
 Quantification of ubiquitinated protein levels in extracts from *N. benthamiana* leaves transiently expressing *pBin+DsRed-RNAi*, *MtVAMP721e-RNAi+DsRed-RNAi*, *CST+DsRed-RNAi*, and *CST+MtVAMP721e-RNAi*. Each bar represents the mean of three biological replicates ± SE. Statistically significant difference between control (*pBin+DsRed-RNAi*) and treatments (*MtVAMP721e-RNAi+DsRed-RNAi*, *CST+DsRed-RNAi* and *CST+MtVAMP721e-RNAi*) is indicated by asterisks (Student's *t*-test: ****P* < 0.001). For original blot see Supplemental Figure 5.

protein in this treatment. In the same leaf the green signal was reduced by 10% (Figure 6C), which is in accordance with the reduction in photosynthesis-related gene expression (Supplemental Figure 3C). Because DsRed protein turnover is supposedly mediated by the proteasome (Verkhusha et al., 2003), these results support the interpretation that in the *C+Vi* treated leaves the 26S proteasome activity is reduced.

Protein Ubiquitination Levels Are Specifically Increased in *C+Vi* Agroinfiltrated Leaves

Proteins are targeted for degradation by protein ubiquitination after which the proteins are recognized by the regulatory particle of the 26S proteasome, which delivers the ubiquitinated protein to the proteasome core for protein degradation. If protein degradation is indeed inhibited in leaves expressing *C+Vi*, for instance because of inactivity of the 26S proteasome, this is expected to result in a higher level of ubiquitinated proteins. We therefore analyzed protein extracts from the leaves from the different treatments for protein ubiquitination levels, using Western blotting with a ubiquitin-specific antibody. As multiple proteins are targeted for ubiquitination and multiple ubiquitins are attached to the same protein, the signals of ubiquitinated proteins on a Western blot are not distinct but diffuse, covering many masses. The signal of ubiquitinated proteins from extracts with the different treatments was quantified and corrected for small differences in loading of the samples as determined by Coomassie brilliant blue (CBB) staining of replicate gels. Results showed that indeed, the signal in the extracts from leaves with *C+Vi* was 1.8-fold higher than that in the extracts from leaves with *C+Di* (Figure 7, for original Western blot see Supplemental Figure 5). The increased levels of ubiquitinated proteins in *C+Vi* agroinfiltrated leaves does indeed suggest that proteasome function is impaired by this combined treatment. Subsequently, we tried to investigate the possible cause of proteasome inhibition in *C+Vi* treatment.

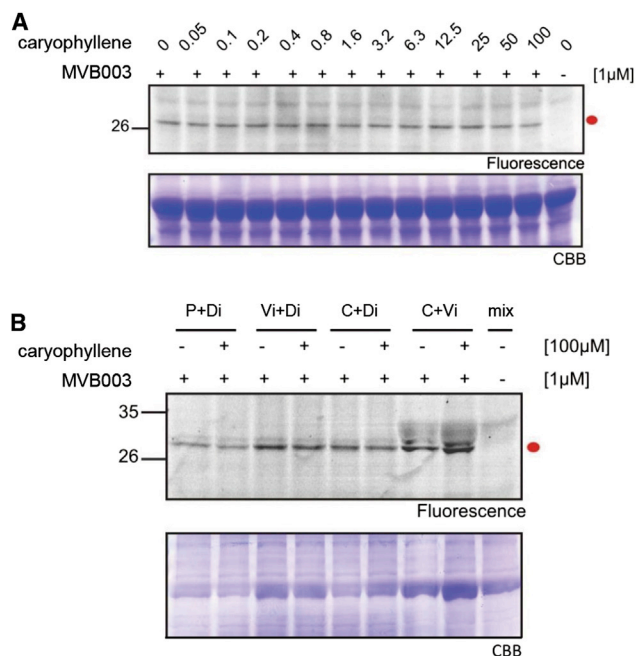


Figure 8. Proteasome Activity Assays.

(A) Proteasome activity is not inhibited by caryophyllene. Top: fluorescence of proteasome-associated protease activity by MVB003 fluorescent labeling in *N. benthamiana* leaf extracts with increasing amount of caryophyllene (0–100 μ M). Bottom: CBB staining of the gel showing sample loading.

(B) Proteasome activity is not lower in C+Vi agroinfiltrated leaves. Top: protein was isolated from *N. benthamiana* leaves agroinfiltrated with *pBin+DsRed-RNAi* (P+Di), *MtVAMP721e-RNAi+DsRed-RNAi* (Vi+Di), *CST+DsRed-RNAi* (C+Di), and *CST+ MtVAMP721e-RNAi* (C+Vi), and proteasome-related protease activity was visualized using MVB003 fluorescent labeling, with (+) or without (–) 100 μ M caryophyllene. Bottom: CBB staining of the gel showing sample loading.

Caryophyllene Does Not Inhibit 20S Proteasome Activity in *In Vitro* Assays

We tested whether caryophyllene can affect protease activity of the proteasome directly in an *in vitro* assay. The protease activity of the proteasome can be monitored using a fluorescent probe (MVB003) which covalently links to the active sites of the caspase-like (β 1), trypsin-like (β 2), and chymotrypsin-like (β 5) proteasome catalytic subunits that are part of the 20S core particle (Kolodziejek et al., 2011). Thus, fluorescent labeling by MVB003 of these proteases can be used as a measure of proteasome activity in a protein extract. Proteasome fractions were obtained from *N. benthamiana* leaves and incubated with the MVB003 probe combined with increasing amounts of caryophyllene. Results show that the labeling of the protease activity in the proteasome was not affected by caryophyllene up to a concentration of 100 μ M in these *in vitro* assays (Figure 8A).

No Reduced 20S Proteasome Activity in Extracts from C+Vi Agroinfiltrated Leaves

While no indications were found that caryophyllene directly affects protease activity of the 20S proteasome, it may be possible that caryophyllene has an indirect effect on proteasome function,

which may require a longer time. For instance, part of the caryophyllene in the cell may be converted to caryophyllene oxide, a compound which was shown previously to cause the formation of reactive oxygen species (Park et al., 2011). Oxidative damage is known to cause disassociation of the 19S and 20S particles, whereby the 20S proteasome remains functional and may lead to 19S inactivation by kinase activity (Lee et al., 2010). Therefore, we tested whether protein extracts from the leaves agroinfiltrated with either C+Di, C+Vi, Vi+Di, or P+Di showed signs of reduced protease activity. Proteasome-containing protein fractions were prepared as described previously (see Methods) and the proteasome activity in the extracts was tested with and without additional 100 μ M caryophyllene. Results showed that the proteasome activity in leaves with C+Vi was not lower than that in leaves from any of the other treatments and, again, activity was not influenced by the addition of caryophyllene (Figure 8B). We did note a trend of higher labeling of proteasomes in the C+Vi fractions, suggesting a higher level of proteasome particles in these samples (Figure 8B). This is in agreement with the higher expression of proteasome-related genes in the C+Vi leaves (Figure 5), but still raises the question as to why the level of ubiquitinated proteins is elevated in these samples (Figure 7).

General oxidative damage may result in protein carbonylation, and carbonyl moieties allow for derivatization with 2,4-dinitrophenylhydrazine (DNPH), which leads to the formation of a stable dinitrophenylhydrazone (DNP) product. Such modified proteins may be separated by PAGE followed by the identification of the DNP moieties of the protein on Western blots using anti-DNP antibodies, and such OxyBlots™ may be used for determination of total protein carbonyl formation (Xiong et al., 2007). However, analysis of proteins by the OxyBlot procedure did not give any indication of increased oxidative damage in the C+Vi treated leaves (Supplemental Figure 6).

Combined, these assays show that there are indications neither of reduced proteasome levels nor protease activity, and no trace of increased oxidative protein damage was found in C+Vi treated leaves.

Other Terpene Synthases Also Increase Protein Stability

To test whether inhibition of vesicle fusion by *MtVAMP721e-RNAi* can be used to boost production of other terpenes, we repeated the experiment with a linalool synthase (plastid-targeted FaNES, cloned from strawberry). Transient expression of *FaNES* (F) in *N. benthamiana* leaves results in the emission of the monoterpene linalool into the headspace (Figure 9A). When *FaNES* expression was combined with *MtVAMP721e-RNAi* expression (F+Vi), the linalool production was enhanced about eight-fold (Figure 9A), similar to the stimulatory effect of Vi on caryophyllene emissions (Figures 2 and 6A). Previously, it was shown that part of the linalool produced in leaves of transgenic plants is converted to glycosylated linalool products (Lücker et al., 2001; Aharoni et al., 2003), but linalool captured in these soluble products can be released by glycosidase treatment. Extracts isolated from leaves agroinfiltrated with F+Vi were treated with glycosidases, and the volatiles released by this treatment were quantified by gel chromatography–mass spectrometry (GC–MS) analysis. Results indicated that the

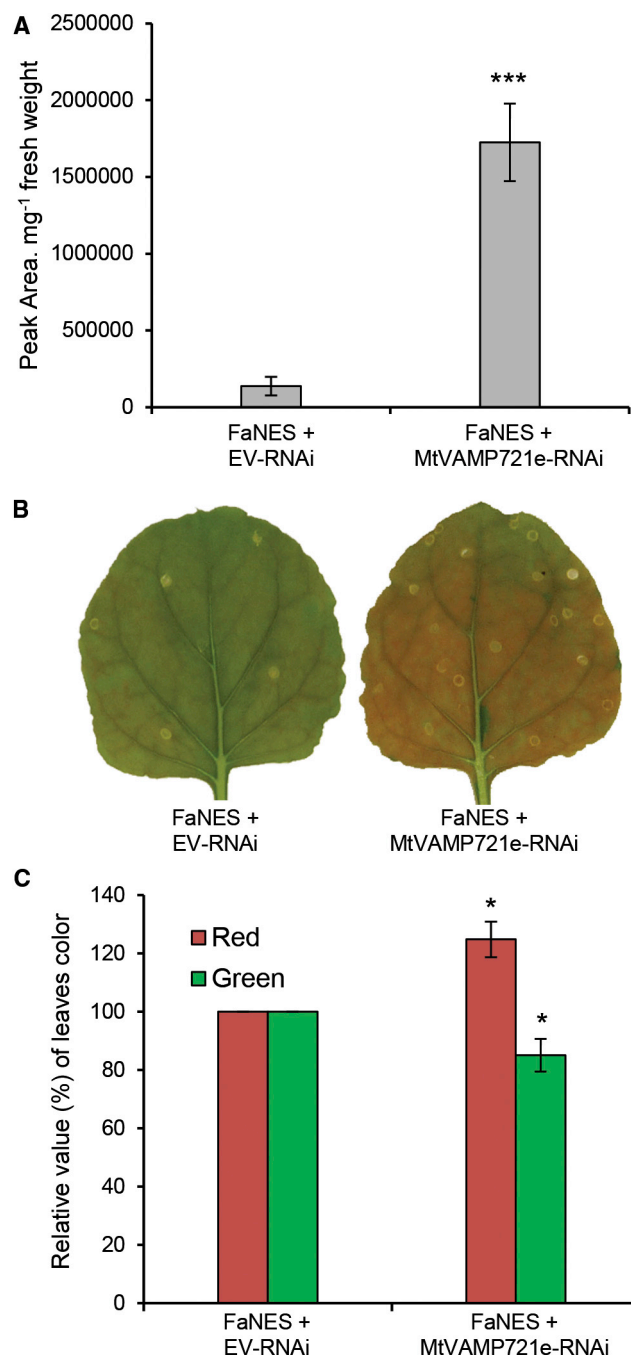


Figure 9. Linalool Emission and DsRed Protein Stability in *FaNES+MtVAMP721e-RNAi* Agroinfiltrated Leaves.

(A) Linalool emission in leaves agroinfiltrated with *FaNES+EV-RNAi* and *FaNES+MtVAMP721e-RNAi*.

(B) Coloration of leaves 7 days post agroinfiltration with *FaNES+EV-RNAi* and *FaNES+MtVAMP721e-RNAi*.

(C) Quantification of relative red and relative green signal intensities in (B). In (A) and (C), each bar represents the mean of three biological replicates \pm SE. Statistically significant differences between *FaNES+EV-RNAi* and *FaNES+MtVAMP721e-RNAi* are indicated by asterisks (Student's *t*-test; * $P < 0.05$; *** $P < 0.001$).

accumulation of glycosylated linalool products also was boosted by the *F+Vi* treatment compared with the *F+Ei* treatment (data not shown). The boosting of the linalool production correlated with

increased stability of the DsRed marker protein, as the *F+Vi* treatment resulted in more red leaves than did the *F+Ei* treatment (Figure 9B and 9C). Combined, these results show that both sesquiterpene and monoterpene can be boosted when VAMP72-mediated vesicle fusion is inhibited. In addition, for linalool we tested whether the *in vitro* proteasome activity can be inhibited by linalool, but up to a concentration of 100 μ M linalool had no effect on protease labeling (Supplemental Figure 7).

DISCUSSION

Strong Interaction between Caryophyllene Production and Inhibition of VAMP72

Although this study started with the question of whether vesicles are involved in the transport of volatile terpenes, the results were not conclusive regarding a direct role of vesicles in terpene transport. Instead we found an unexpected strong interaction between ectopic expression of a terpene synthase (CST or *FaNES*) and inhibition of *VAMP72* genes through coexpression with *MtVAMP721e-RNAi* (*Vi*), resulting in higher caryophyllene or linalool emission, respectively (Figures 2 and 6). Transcript analysis showed that the treatment of *C+Di* or *Vi+Di* resulted in only a limited transcriptional response compared with the control treatment (*P+Di*) (Figure 3A and 3B) and that the *Vi* is able to suppress multiple *VAMP72* genes in *N. benthamiana* (Supplemental Figure 1). However, the RNA-seq analysis of the *C+Vi* treatment showed a stronger transcriptional response than that of *C+Di* and *Vi+Di* combined (Figure 3A and 3B). Most pronounced is the coordinated upregulation of multiple genes related to the proteasome base, core, and lid in *C+Vi* (Figure 5). However, the higher expression of the proteasome-related genes does not result in a higher protein turnover, but rather coincides with an apparent increase in protein stability (increased DsRed, Figure 6; increased level of ubiquitinated proteins, Figure 7). An increase in stability of proteins in the caryophyllene biosynthesis pathway may explain the higher emission of caryophyllene in the *C+Vi* compared with the *C+Di* treatment (Figure 2)

Qualitatively, similar results were obtained by combining linalool synthase (*F*) with *Vi*. The *F+Vi* treatment resulted in both increased linalool emission and accumulation of linalool-derived glycosides (Figure 9), indicating that indeed overall production is increased. Because DsRed accumulation is also increased in *F+Vi* leaves, this is indicative of a similar effect on protein stability in *F+Vi* as observed for the *C+Vi* treatments.

Feedback Regulation of Proteasome Genes in *N. benthamiana*?

We interpret the coordinated upregulation of the proteasome genes in the *C+Vi* leaves as the result of a proteasome malfunction. Studies in mammals and yeast have shown that proteasome gene expression is under feedback control of transcription factor(s) which are target(s) for proteasome-mediated degradation (Kobayashi and Yamamoto, 2005; Villeneuve et al., 2010). As a result, impaired proteasome function causes stabilization of these transcription factors, resulting in an upregulation of proteasome genes in an attempt to maintain the homeostasis in proteasome functionality (Meiners et al., 2003; Dreger et al., 2010). Presumably, proteasome homeostasis in plants is under

SNARE-RNAi Boosts Terpene Production

a similar transcriptional feedback control. The apparent impairment of proteasome function by the C+Vi treatment could therefore explain the upregulation of the expression of proteasome-associated genes in our study (Figure 5 and Supplemental Table 8). In yeast the *Ump1* gene is responsible for *de novo* 20S proteasome formation and if there is a coordinated upregulation of proteasome genes, this gene is most likely also involved (Ramos et al., 1998). Indeed, besides the proteasome lid, base, and core component genes, the closest homolog of *Ump1* in *N. benthamiana* (*NbS00012508g0011.1*) was also upregulated two-fold in the C+Vi treated leaves.

The upregulation of the proteasome genes in C+Vi leaves seems not to be sufficient to fully restore proteasome functionality, as the level of ubiquitinated proteins is still elevated in these leaves (Figure 7) and our marker protein DsRed also shows higher levels of accumulation in C+Vi (Figure 6). Recently it was shown that in *Arabidopsis* the genes encoding components of the 26S proteasome are under control of the NAC transcription factor ANAC078 (Yabuta et al., 2011; Nguyen et al., 2013). We blasted the sequence of ANAC078 to the *N. benthamiana* proteome to identify the putative homologs of ANAC078 in *N. benthamiana*. The two targets with highest homology to ANAC078 (*NbS00000666g0007* and *NbS00038001g0007*) did not display any differential transcriptional activity in the leaves with C+Vi treatment. Therefore, when either of these proteins is indeed involved in proteasome-related gene expression in *N. benthamiana*, the effect of the C+Vi treatment on upregulation of proteasome gene expression must be mediated by effects on the stability of these ANAC078 homologs.

Additional Indirect Indications of Proteasome Impairment in C+Vi Agroinfiltrated Leaves

The transcriptional activity of the endogenous *NbCST* genes was down in C+Vi compared with P+Di (Supplemental Figure 4). Moreover, the RNA-seq analysis indicated that the C+Vi treatment resulted in downregulation of the expression of multiple genes of the MVA pathway (*HMGS*, *HMGR*, *IDI*) and the MEP pathway (*MCS*, *HDS*, *IDI*) and the first step toward sesquiterpene biosynthesis (*FDS*) (Supplemental Figure 8). These effects were specific for C+Vi, as no downregulation of these genes was observed in either C+Di or Vi+Di. Although the transcriptional activity of *CST* was slightly higher in the C+Vi than in the C+Di treatment (Figure 4), we assumed that this alone cannot account for the five-fold increase in caryophyllene emission by leaves agroinfiltrated with C+Vi. The higher caryophyllene emissions may therefore be explained by a decreased turnover of enzymes in the caryophyllene biosynthesis pathway. This inferred increased stability of caryophyllene biosynthesis enzymes may relate to the apparent proteasome impairment in the C+Vi treatment.

Recently it was reported that the expression of photosynthesis genes is mainly controlled by the transcriptional repressor PIF3, for which protein stability is regulated by ubiquitination and proteasome-mediated degradation (Liu et al., 2013). Impaired proteasome activity could result in stabilization of the *N. benthamiana* PIF3 homolog, resulting in enhanced suppression of photosynthesis genes, as was observed for the

C+Vi treatment (Supplemental Figure 3C). The reduced photosynthesis gene includes reduced activity of magnesium protoporphyrin O-methyltransferase (*NbS00045366g0002.1*), a key enzyme in protochlorophyllide biosynthesis, which may explain the reduced chlorophyll content in C+Vi agroinfiltrated leaves (Figure 6C).

Decreased Interaction between Proteasome Lid and Core in C+Vi Treated Leaves?

While there are multiple indirect (Figures 2, 6, and 9; Supplemental Figure 8) and direct indications (Figures 5 and 7; Supplemental Figure 5) of a diminished turnover of (ubiquitinated) proteins by the proteasome in the C+Vi leaves, it is not clear where this apparent inhibition of proteasome function takes place. For instance, the *in vitro* assay of protease activity of isolated proteasome fractions from C+Vi did not show indications of impaired protease activity in the C+Vi samples (Figure 8). In fact, the results from the *in vitro* proteasome activity assays hints at increased rather than decreased proteasome-related protease activity in the C+Vi agroinfiltrated leaves (Figure 8). Also, ectopic expression of *CST* without *Vi* did not result in proteasome impairment and, moreover, in an *in vitro* assay caryophyllene did not inhibit the protease activity in isolated proteasome fractions (Figure 8). Therefore, there is a seeming discrepancy between the proteasome activity as measured in the *in vitro* assays and the reduced degradation of ubiquitinated proteins *in planta*. These seemingly conflicting results may still be explained when we assume that the delivery of ubiquitinated proteins by the regulatory particle (lid) to the proteasome core (20S) of the 26S proteasome is somehow impaired in leaves agroinfiltrated with C+Vi.

CONCLUDING REMARKS

More research will be needed in future to investigate whether the interaction between proteasome lid and core is the basis for proteasome impairment in C+Vi treatment. Moreover, it needs to be determined whether caryophyllene and linalool have a specific role in this process. Due to the unexpected effects of inhibition of vesicle transport, we remain cautious about the role of vesicles in the transport of terpenes. Analysis of a direct effect of vesicle fusions on terpene emission will require time-resolved caryophyllene emission measurements, combined with an inducible *VAMP72-RNAi* construct. Although at present the role of vesicles in terpene transport has not been resolved, our study does show for the first time that terpene production may actually be improved by inhibition of vesicle fusion. Moreover, as proteasomes are targets in cancer research (Almond and Cohen, 2002; Adams, 2004; Yang et al., 2006; Kupperman et al., 2010; Schumacher et al., 2010), our findings may also provide new leads for the role of terpenes in medical research.

METHODS

Vector Construction

35S:DsRed-RNAi

The Gateway pK7GWIWG2(II)-Q10::DsRED binary vector which contains the red fluorescent marker DsRED1 under the constitutive *Arabidopsis Ubiquitin10* promoter was obtained from Dr. Sergey Ivanov (Ivanov et al., 2012). To construct a *DsRed-RNAi* construct, a 223 bp fragment was amplified using the primer pair attB1-DsRed-F/attB2-DsRed-R

(Supplemental Table 9) using the pK7GWIWG2(II)-Q10::DsRED vector as template. The amplicon was subcloned into the pDONR221 vector (Invitrogen Life Technologies, Carlsbad, CA, USA) using the BP Clonase II enzyme mix (Invitrogen) to generate an entry vector pDONR221-DsRed. In a subsequent step, the RNAi fragments were cloned into the pK7GWIWG2(II)-Q10::DsRED vector through LR recombination (Invitrogen). The vector was transferred to *Agrobacterium tumefaciens* AGL-0 by electroporation.

35S:MtVAMP721e-RNAi and 35S:EV-RNAi

MtVAMP721e-RNAi and EV-RNAi, which both contain the DsRed reporter gene, were kindly provided by Dr. Sergey Ivanov and Prof. Ton Bisseling (Ivanov et al., 2012).

35S:CST

Genomic DNA was extracted from *Arabidopsis thaliana* (L.) Heynh (Col.0) leaves by the cetyltrimethylammonium bromide method (Chen et al., 2008). A 2160 bp genomic DNA fragment containing six introns from start codon to stop codon of caryophyllene synthase (At5g23960) was amplified by PCR using the primer pair CST-F/CST-R (Supplemental Table 9). The primers used introduce NcoI and NotI restriction sites, which were used for cloning into ImpactVectorpIV1A_2.1, which contains the CaMV35S promoter and Rbcs1 terminator (<http://www.wageningenur.nl/en/show/Productie-van-farmaceutische-en-industriele-eiwitten-door-planten.htm>). The resulting pIV1A_2.1/CST was cloned into the PinPlus binary vector using LR recombination (Invitrogen) (van Engelen et al., 1995). The PinPlus construct containing the 35S:CST was transferred to *A. tumefaciens* AGL-0 using electroporation.

35S:FaNES

The strawberry linalool/nerolidol synthase, FaNES, with a synthetic intron (Yang et al., 2008) was cloned into ImpactVectorpIV1A_2.4, which contains a CaMV35S promoter, plastid targeting signal, and Rbcs1 terminator (<http://www.wageningenur.nl/en/show/Productie-van-farmaceutische-en-industriele-eiwitten-door-planten.htm>) (obtained from Jan G. Schaart, Plant Breeding, Wageningen University). pIV1A_2.4/FaNES was cloned into the PinPlus binary vector using LR recombination (Invitrogen) (van Engelen et al., 1995).

N. Benthamiana VAMP72 Gene Sequence Analysis

To identify the *N. benthamiana* VAMP72 genes, we used *Arabidopsis* VAMP72 genes to BLAST against the *N. benthamiana* genome sequence, which resulted in 14 NbVAMP72 genes. The percentage of sequence similarity between MtVAMP721e and NbVAMP72s was calculated using BLAST (Altschul et al., 1997) at the NCBI website (<http://blast.ncbi.nlm.nih.gov/>).

Transient Expression Assays in N. Benthamiana

Transient expression in leaves of *N. benthamiana* was done as previously reported (Ting et al., 2013). The total dosage of *A. tumefaciens* within each experiment was kept constant for the different gene combinations. *N. benthamiana* leaves were infiltrated with *Agrobacterium* containing the following expression constructs: (1) pBin+DsRed-RNAi, (2) MtVAMP721e-RNAi+DsRed-RNAi, (3) CST+DsRed-RNAi, (4) CST+MtVAMP721e-RNAi, (5) CST+EV-RNAi, (6) FaNES+MtVAMP721e-RNAi, and (7) FaNES+EV-RNAi (six plants per construct, one leaf per plant). Infiltrated leaves were harvested 7 days post agroinfiltration. Two leaves per sample were pooled, resulting in three biological replicates for each treatment.

Headspace Trapping and Analysis of Volatiles by GC-MS

The volatile headspace of the agroinfiltrated *N. benthamiana* leaves was analyzed by placing leaves in a vial with water to prevent dehydration, and placing the vial in a 1-l glass jar from which volatiles were collected for 30 min (between 1:45 pm and 2:15 pm) using dynamic headspace trapping as described (Houshyani et al., 2013). The headspace samples were analyzed by GC-MS as described (Houshyani et al., 2013). Terpenoids were identified by comparison of mass spectra and retention time with authentic standards: caryophyllene (Sigma-Aldrich, St Louis, MO, USA) and linalool (Fluka, Buchs, Switzerland). Quantification of terpene levels was accomplished by determining the

peak area of the characteristic *m/z* (133 for caryophyllene and 71 + 93 for linalool).

RNA Isolation

After harvest, leaves were immediately frozen in liquid nitrogen and ground to a fine powder for RNA isolation. RNA was extracted using the RNeasy® Plant Mini kit (Qiagen, Hilden, Germany) with on-column RNase-Free DNase digestion (Qiagen). The quantity and quality of RNA for qRT-PCR was determined using a NanoDrop (NanoDrop Technologies, Wilmington, DE, USA) and agarose gel electrophoresis. For RNA-seq analysis, the RNA quality was checked using an Agilent 2100 Bioanalyzer (Agilent, Santa Clara, CA, USA).

qRT-PCR

cDNA was transcribed from 1 µg of RNA using the iScript cDNA Synthesis kit (Bio-Rad, Hercules, CA, USA) and diluted 20-fold before use as template for qRT-PCR. A gene-specific primer pair NbVAMP72c-F/NbVAMP72c-R was used for PCR. GADPH was used for normalization (Torres-Barceló et al., 2008) (Supplemental Table 9). Each PCR reaction mixture contained 1 µl of cDNA template, 2 µl of each primer (3 µM), 10 µl of iQ™ SYBR® Green Supermix master mix (Bio-Rad), and 5 µl of deionized water. The PCR was performed in the iCycler iQ5 system (Bio-Rad) using a three-step temperature program: (1) 95°C for 3 min, (2) 40 cycles of 95°C for 10 s, and 55°C for 30 s, and (3) 95°C for 1 min, followed by melting-curve analysis from 65°C to 95°C. Relative expression values were calculated using the efficiency δ Ct (cycle threshold) method (Livak and Schmittgen, 2001).

RNA Sequencing and Data Analysis

Construction of the cDNA libraries and subsequent Illumina paired-end sequencing (Illumina HiSeq™ 2000) was performed by BGI, China. The processed and raw data are available from the Gene Expression Omnibus (GEO: GSE60061). The processed reads were assembled by BGI, using the available *N. benthamiana* genome sequence as a template (Bombarely et al., 2012), which was carried out using the SOAPaligner/SOAP2 program with the default settings (Li et al., 2009). The gene expression level was calculated using the RPKM (reads per kb per million reads) method (Mortazavi et al., 2008). We used an FDR ≤ 0.05 and the absolute value of \log_2 Ratio ≥ 1 as the threshold to select significance of gene expression differences. Differentially expressed genes were then used for GO functional analysis, using Blast2GO (Conesa et al., 2005). For pathway analysis, we mapped all differentially expressed genes to terms in the KEGG (Ogata et al., 1999). MapMan was used to visualize gene expression changes, using the tomato pathways (<http://mapman.gabipd.org/web/guest/mapmanstore>) (Thimm et al., 2004).

Analysis of Proteasome Activity

Ubiquitinated Protein Western Blot

26S protein ubiquitination level was inferred from semi-quantified ubiquitinated protein levels on Western blots. Liquid nitrogen frozen agroinfiltrated leaf material was fractured with two (5/35) metal bullets by a dismembrator at 30 sweeps/s. Proteins were extracted in a fresh 50 mM Tris-HCl (pH 8; Biomol, Hamburg, Germany) buffer of 4°C with 5 mM dithiothreitol (DTT), 2 mM SDS (Fisher Scientific, Waltham, MA, USA), and a complete protease inhibitor cocktail tablet (complete that also delivers 1 mM EDTA; Roche Diagnostics Nederland, Flevoland, the Netherlands) (adapted from Lough et al., 1998). Samples were prepared for SDS-PAGE through a 4% stacking gel and 7.5% running gel (from 30% acrylamide/bis; 37.5:1; Bio-Rad). Gels were stained with CBB according to Wondrak (2001) to judge the loading equality or were blotted onto a 0.45 µm pore polyvinylidene difluoride (PVDF) membrane (Thermo Scientific, Rockford, IL, USA) at 4°C under a constant voltage (90 V; 20 mA/blot) for 60 min. Excess protein was discarded from the blot with Tris-buffered saline (TBS). Blocking buffer (TBS with 5% non-fat dried milk; FrieslandCampina, Utrecht, the Netherlands) was applied to the

blot for 60 min at room temperature. Ubiquitinated proteins were targeted by polyclonal anti-UBQ11 rabbit antibodies (antibodies-online.com, Aachen, Germany). Repeated washing with TBS, incubation with secondary anti-rabbit antibodies from goat (GE Healthcare, Buckinghamshire, UK), and further washing prepared the incubation with luminol (GE Healthcare). Luminol oxidation and excitation was catalyzed by horseradish peroxidase ligated to the secondary antibodies for 1 min. An Acton Pixis 1024 camera (Princeton Instruments, Trenton, NJ, USA), air-cooled to -78°C , recorded the ubiquitin-derived luminescence for 20 s of exposure time. Gray-scale CBB and luminescence signals were semi-quantified with the Measure Mean gray value function of the software program ImageJ.

Protein Oxidation Western Blot

As a source of 26S proteasome disintegration, oxidative damage to proteins was probed. Using the OxyBlot™ kit (Merck, Hesse, Germany), protein carbonylation was visualized on a Western blot. Carbonyls were derivatized with 2,4-DNPH in extension to the protein extraction. To this end, 5% SDS was dissolved in the protein extract prior to an equal volume of a low pH buffer with 2,4-DNPH (according to the instruction manual). With the addition of neutralization buffer after 15 min the reaction to DNP was discontinued. A 100× dilution of rabbit primary anti-DNP antibodies (OxyBlot) in blocking buffer was applied to the Western blot that was prepared, processed, and examined as described for the ubiquitinated protein Western blot.

Proteasome Activity Measurements

Four leaves of each sample (approximately 2.5 g of tissue) were ground in 5 ml buffer containing 2 mM DTT and 67 mM Tris (pH 7.5). Extracts were centrifuged and filtered through a 0.22 μm PVDF membrane until a clear sample was produced. Protein samples were labeled at room temperature with 1 μM MVB003 for 2 h in a total volume of 60 μl (Kolodziejek et al., 2011). For the competition assay, samples were pre-incubated with different concentrations of caryophyllene (Sigma-Aldrich) or linalool (Fluka) for 30 min followed by labeling with MVB003 for 2 h. An equal amount of all samples were combined and 0.5%–1% dimethylsulfoxide was added to generate the no-probe control (NPC). Reaction was stopped by boiling the samples in 1× gel loading buffer containing SDS. Protein samples were separated on 12% SDS-PAGE protein gels and fluorescently labeled proteins were detected by in-gel fluorescence scanning using the Typhoon FLA9000 with the following settings: 532 nm laser, BPG1 filter, and 1000 PTM sensitivity.

SUPPLEMENTAL INFORMATION

Supplemental Information is available at *Molecular Plant Online*.

FUNDING

H-M.T. was funded by the graduate school of Experimental Plant Sciences (EPS). We thank the Max Planck Society for financial support.

ACKNOWLEDGMENTS

We thank Dr. Sergey Ivanov and Prof. Ton Bisseling for providing 35S:*MtVAMP721e-RNAi* and 35S:*EV-RNAi* constructs. We thank Jan G. Schaart for providing the pV1A_2.4/FaNES construct. We would like to thank Francel W.A. Verstappen, Iris Kappers, Geert Stoop, Roland Mumm, Berhane Weldegergis, and Peter Tóth for their assistance with headspace trapping and GC-MS analysis. We thank Desalegn Woldes Etalo for help with MS data analysis, Esmer Jongedijk for help with the terpene biosynthesis pathway figure, Ralph Bours for help with ImageJ software, and Giovanni Melandri who shared the OxyBlot™ kit with us. No conflict of interest declared.

Received: July 30, 2014

Revised: January 7, 2015

Accepted: January 9, 2015

Published: January 15, 2015

REFERENCES

- Adams, J. (2004). The development of proteasome inhibitors as anticancer drugs. *Cancer Cell* **5**:417–421.
- Aharoni, A., Giri, A.P., Deuerlein, S., Griepink, F., de Kogel, W.J., Verstappen, F.W., Verhoeven, H.A., Jongma, M.A., Schwab, W., and Bouwmeester, H.J. (2003). Terpenoid metabolism in wild-type and transgenic *Arabidopsis* plants. *Plant Cell* **15**:2866–2884.
- Almond, J., and Cohen, G. (2002). The proteasome: a novel target for cancer chemotherapy. *Leukemia* **16**:433–443.
- Altschul, S.F., Madden, T.L., Schäffer, A.A., Zhang, J., Zhang, Z., Miller, W., and Lipman, D.J. (1997). Gapped BLAST and PSI-BLAST: a new generation of protein database search programs. *Nucleic Acids Res.* **25**:3389–3402.
- Bombarely, A., Rosli, H.G., Vrebalov, J., Moffett, P., Mueller, L.A., and Martin, G.B. (2012). A draft genome sequence of *Nicotiana benthamiana* to enhance molecular plant-microbe biology research. *Mol. Plant Microbe Interact.* **25**:1523–1530.
- Chen, H.J., Wen, I.C., Huang, G.J., Hou, W.C., and Lin, Y.H. (2008). Expression of sweet potato asparaginyl endopeptidase caused altered phenotypic characteristics in transgenic *Arabidopsis*. *Bot. Stud.* **49**:109–117.
- Conesa, A., Gotz, S., Garcia-Gomez, J.M., Terol, J., Talon, M., and Robles, M. (2005). Blast2GO: a universal tool for annotation, visualization and analysis in functional genomics research. *Bioinformatics* **21**:3674–3676.
- Dreger, H., Westphal, K., Wilck, N., Baumann, G., Stangl, V., Stangl, K., and Meiners, S. (2010). Protection of vascular cells from oxidative stress by proteasome inhibition depends on Nrf2. *Cardiovasc. Res.* **85**:395–403.
- Eckstein-Ludwig, U., Webb, R.J., Van Goethem, I.D., East, J.M., Lee, A.G., Kimura, M., O'Neill, P.M., Bray, P.G., Ward, S.A., and Krishna, S. (2003). Artemisinins target the SERCA of *Plasmodium falciparum*. *Nature* **424**:957–961.
- Filippini, F., Rossi, V., Galli, T., Budillon, A., D'Urso, M., and D'Esposito, M. (2001). Longins: a new evolutionary conserved VAMP family sharing a novel SNARE domain. *Trends Biochem. Sci.* **26**:407–409.
- Fujimoto, M., and Ueda, T. (2012). Conserved and plant-unique mechanisms regulating plant post-Golgi traffic. *Front. Plant Sci.* **3**:197.
- Gershenson, J., and Dudareva, N. (2007). The function of terpene natural products in the natural world. *Nat. Chem. Biol.* **3**:408–414.
- Holopainen, J.K., and Gershenson, J. (2010). Multiple stress factors and the emission of plant VOCs. *Trends Plant Sci.* **15**:176–184.
- Houshyani, B., Assareh, M., Busquets, A., Ferrer, A., Bouwmeester, H.J., and Kappers, I.F. (2013). Three-step pathway engineering results in more incidence rate and higher emission of nerolidol and improved attraction of *Diadegma semiclausum*. *Metab. Eng.* **15**:88–97.
- Ivanov, S., Fedorova, E.E., Limpens, E., De Mita, S., Genre, A., Bonfante, P., and Bisseling, T. (2012). Rhizobium-legume symbiosis shares an exocytotic pathway required for arbuscule formation. *Proc. Natl Acad. Sci. USA* **109**:8316–8321.
- Kobayashi, M., and Yamamoto, M. (2005). Molecular mechanisms activating the Nrf2-Keap1 pathway of antioxidant gene regulation. *Antioxid. Redox Signal.* **7**:385–394.
- Kolodziejek, I., Misas-Villamil, J.C., Kaschani, F., Clerc, J., Gu, C., Krahn, D., Niessen, S., Verdoes, M., Willems, L.I., Overkleeft, H.S., et al. (2011). Proteasome activity imaging and profiling characterizes bacterial effector syringolin A. *Plant Physiol.* **155**:477–489.
- Kupperman, E., Lee, E.C., Cao, Y., Bannerman, B., Fitzgerald, M., Berger, A., Yu, J., Yang, Y., Hales, P., Bruzzese, F., et al. (2010).

- Evaluation of the proteasome inhibitor MLN9708 in preclinical models of human cancer. *Cancer Res.* **70**:1970–1980.
- Kwon, C., Bednarek, P., and Schulze-Lefert, P.** (2008). Secretory pathways in plant immune responses. *Plant Physiol.* **147**:1575–1583.
- Lang, T., and Jahn, R.** (2008). Core proteins of the secretory machinery. *Handb. Exp. Pharmacol.* **184**:107–127.
- Lee, S.H., Park, Y., Yoon, S.K., and Yoon, J.B.** (2010). Osmotic stress inhibits proteasome by p38 MAPK-dependent phosphorylation. *J. Biol. Chem.* **285**:41280–41289.
- Lev, S.** (2010). Non-vesicular lipid transport by lipid-transfer proteins and beyond. *Nat. Rev. Mol. Cell Biol.* **11**:739–750.
- Li, R., Yu, C., Li, Y., Lam, T.W., Yiu, S.M., Kristiansen, K., and Wang, J.** (2009). SOAP2: an improved ultrafast tool for short read alignment. *Bioinformatics* **25**:1966–1967.
- Liu, X., Chen, C.Y., Wang, K.C., Luo, M., Tai, R., Yuan, L., Zhao, M., Yang, S., Tian, G., Cui, Y., et al.** (2013). PHYTOCHROME INTERACTING FACTOR3 associates with the histone deacetylase HDA15 in repression of chlorophyll biosynthesis and photosynthesis in etiolated *Arabidopsis* seedlings. *Plant Cell* **25**:1258–1273.
- Livak, K., and Schmittgen, T.** (2001). Analysis of relative gene expression data using real-time quantitative PCR and the 2^{-ΔΔC_T} method. *Methods* **25**:402–408.
- Lough, T.J., Balmori, E., Beck, D.L., and Forster, R.L.** (1998). Western analysis of transgenic plants. In *Plant Virology Protocols*, G.D. Foster and S.C. Taylor, eds. (New York: Springer), pp. 447–451.
- Lücker, J., Bouwmeester, H.J., Schwab, W., Blaas, J., Van Der Plas, L.H.W., and Verhoeven, H.A.** (2001). Expression of Clarkia S linalool synthase in transgenic petunia plants results in the accumulation of S-linalyl-d-glucopyranoside. *Plant J.* **27**:315–324.
- Meiners, S., Heyken, D., Weller, A., Ludwig, A., Stangl, K., Klotzel, P.M., and Krüger, E.** (2003). Inhibition of proteasome activity induces concerted expression of proteasome genes and *de novo* formation of mammalian proteasomes. *J. Biol. Chem.* **278**:21517–21525.
- Mortazavi, A., Williams, B.A., McCue, K., Schaeffer, L., and Wold, B.** (2008). Mapping and quantifying mammalian transcriptomes by RNA-Seq. *Nat. Methods* **5**:621–628.
- Nguyen, H.M., Schippers, J.H., Góni-Ramos, O., Christoph, M.P., Dortay, H., van der Hoorn, R.A., and Mueller-Roeber, B.** (2013). An upstream regulator of the 26S proteasome modulates organ size in *Arabidopsis thaliana*. *Plant J.* **74**:25–36.
- Ogata, H., Goto, S., Sato, K., Fujibuchi, W., Bono, H., and Kanehisa, M.** (1999). KEGG: kyoto encyclopedia of genes and genomes. *Nucleic Acids Res.* **27**:29–34.
- Park, K.R., Nam, D., Yun, H.M., Lee, S.G., Jang, H.J., Sethi, G., Cho, S.K., and Ahn, K.S.** (2011). β-Caryophyllene oxide inhibits growth and induces apoptosis through the suppression of PI3K/AKT/mTOR/S6K1 pathways and ROS-mediated MAPKs activation. *Cancer Lett.* **312**:178–188.
- Ramos, P.C., Höckendorff, J., Johnson, E.S., Varshavsky, A., and Dohmen, R.J.** (1998). Ump1p is required for proper maturation of the 20S proteasome and becomes its substrate upon completion of the assembly. *Cell* **92**:489–499.
- Sanderfoot, A.** (2007). Increases in the number of SNARE genes parallels the rise of multicellularity among the green plants. *Plant Physiol.* **144**:6–17.
- Schumacher, M., Cerella, C., Eifes, S., Chateauvieux, S., Morceau, F., Jaspars, M., Dicato, M., and Diederich, M.** (2010). Heteronemin, a spongian sesterterpene, inhibits TNF alpha-induced NF-kappa B activation through proteasome inhibition and induces apoptotic cell death. *Biochem. Pharmacol.* **79**:610–622.
- Skubatz, H., Kunkel, D.D., Patt, J.M., Howald, W.N., Hartman, T.G., and Meeuse, B.** (1995). Pathway of terpene excretion by the appendix of *Sauromatum guttatum*. *Proc. Natl Acad. Sci. USA* **92**:10084–10088.
- Thimm, O., Bläsing, O., Gibon, Y., Nagel, A., Meyer, S., Krüger, P., Selbig, J., Müller, L.A., Rhee, S.Y., and Stitt, M.** (2004). MAPMAN: a user-driven tool to display genomics data sets onto diagrams of metabolic pathways and other biological processes. *Plant J.* **37**:914–939.
- Ting, H.M., Wang, B., Rydén, A.M., Woittiez, L., van Herpen, T., Verstappen, F.W., Ruyter-Spira, C., Beekwilder, J., Bouwmeester, H.J., and van der Krol, A.** (2013). The metabolite chemotype of *Nicotiana benthamiana* transiently expressing artemisinin biosynthetic pathway genes is a function of *CYP71AV1* type and relative gene dosage. *New Phytol.* **199**:352–366.
- Torres-Barceló, C., Martín, S., Daròs, J.A., and Elena, S.F.** (2008). From hypo- to hypersuppression: effect of amino acid substitutions on the RNA-silencing suppressor activity of the *Tobacco etch potyvirus* HC-Pro. *Genetics* **180**:1039–1049.
- van Engelen, F.A., Molthoff, J.W., Conner, A.J., Nap, J.P., Pereira, A., and Stiekema, W.J.** (1995). pBINPLUS: an improved plant transformation vector based on pBIN19. *Transgenic Res.* **4**:288–290.
- Verkhusha, V.V., Kuznetsova, I.M., Stepanenko, O.V., Zaraisky, A.G., Shavlovsky, M.M., Turoverov, K.K., and Uversky, V.N.** (2003). High stability of *Discosoma* DsRed as compared to *Aequorea* EGFP. *Biochemistry* **42**:7879–7884.
- Villeneuve, N.F., Lau, A., and Zhang, D.D.** (2010). Regulation of the Nrf2-Keap1 antioxidant response by the ubiquitin proteasome system: an insight into cullin-ring ubiquitin ligases. *Antioxid. Redox Signal.* **13**:1699–1712.
- Wondrak, E.M.** (2001). Process for Fast Visualization of Protein, US6319720 B1 (Washington, DC: LLP, P.W.).
- Xiong, Y., Contento, A.L., Nguyen, P.Q., and Bassham, D.C.** (2007). Degradation of oxidized proteins by autophagy during oxidative stress in *Arabidopsis*. *Plant Physiol.* **143**:291–299.
- Yabuta, Y., Osada, R., Morishita, T., Nishizawa-Yokoi, A., Tamoi, M., Maruta, T., and Shigeoka, S.** (2011). Involvement of *Arabidopsis* NAC transcription factor in the regulation of 20S and 26S proteasomes. *Plant Sci.* **181**:421–427.
- Yang, H., Chen, D., Cui, Q.C., Yuan, X., and Dou, Q.P.** (2006). Celastrol, a triterpene extracted from the Chinese “Thunder of God Vine,” is a potent proteasome inhibitor and suppresses human prostate cancer growth in nude mice. *Cancer Res.* **66**:4758–4765.
- Yang, L.-M., Mercke, P., van Loon, J.J., Fang, Z.-Y., Dicke, M., and Jongsma, M.A.** (2008). Expression in *Arabidopsis* of a strawberry linalool synthase gene under the control of the inducible potato PI2 promoter. *Agr. Sci. China* **7**:521–534.
- Zhao, J., and Dixon, R.A.** (2010). The ‘ins’ and ‘outs’ of flavonoid transport. *Trends Plant Sci.* **15**:72–80.